Harnessing the cytotoxic granule exocytosis to augment the efficacy of T-cell-engaging bispecific antibody therapy

Mika Casey,[1] Carol Lee,[1] Sharon M. Hoyte,[1] Rebecca L. Johnston,[1] Wing Yu Kwok,[1] Soi Cheng Law,[2] Maher K. Gandhi,[2] Simon J. Harrison[3,4] and Kyohei Nakamura[1]

[1]Cancer Research Program, QIMR Berghofer Medical Research Institute, Brisbane, Queensland; [2]Mater Research, University of Queensland, Brisbane, Queensland; [3]Clinical Hematology, Peter MacCallum Cancer Center and Royal Melbourne Hospital, Melbourne, Victoria and [4]Sir Peter MacCallum, Department of Oncology, University of Melbourne, Parkville, Victoria, Australia

Correspondence: K. Nakamura
kyohei.nakamura@qimrberghofer.edu.au

Received: October 30, 2023.
Accepted: January 12, 2024.
Early view: January 25, 2024.

https://doi.org/10.3324/haematol.2023.284435

Abstract

T-cell-engaging bispecific antibody (T-BsAb, also known as BiTE) therapy has emerged as a powerful therapeutic modality against multiple myeloma. Given that T-BsAb therapy redirects endogenous T cells to eliminate tumor cells, reinvigorating dysfunctional T cells may be a potential approach to improve the efficacy of T-BsAb. While various immunostimulatory cytokines can potentiate effector T-cell functions, the optimal cytokine treatment for T-BsAb therapy is yet to be established, partly due to a concern of cytokine release syndrome driven by aberrant interferon (IFN)-γ production. Here, we functionally screen immunostimulatory cytokines to determine an ideal combination partner for T-BsAb therapy. This approach reveals interleukin (IL)-21 as a potential immunostimulatory cytokine with the ability to augment T-BsAb-mediated release of granzyme B and perforin, without increasing IFN-γ release. Transcriptome profiling and functional characterization strongly support that IL-21 selectively targets the cytotoxic granule exocytosis pathway, but not pro-inflammatory responses. Notably, IL-21 modulates multiple steps of cytotoxic effector functions including upregulation of co-activating CD226 receptor, increasing cytotoxic granules, and promoting cytotoxic granule delivery at the immunological synapse. Indeed, T-BsAb-mediated myeloma killing is cytotoxic granule-dependent, and IL-21 priming significantly augments cytotoxic activities. Furthermore, *in vivo* IL-21 treatment induces cytotoxic effector reprogramming in bone marrow T cells, showing synergistic anti-myeloma effects in combination with T-BsAb therapy. Together, harnessing the cytotoxic granule exocytosis pathway by IL-21 may be a potential approach to achieve better responses by T-BsAb therapy.

Supplementary File

Supplementary Tables (see excel files)

- **Supplementary Table 1:** The RNA-seq count matrix.
- **Supplementary Table 2:** Differential expression analysis between IL-21-primed and control CD8 T cells.
- **Supplementary Table 3:** Reactome pathway analysis of the genes up-regulated in IL-21-primed CD8 T cells.
- **Supplementary Table 4:** Reactome pathway analysis of the genes down-regulated in IL-21-primed CD8 T cells.

Key Materials and Resources

REAGENT or RESOURCE	Source/ References
Experimental models: Mouse strains	
C57BL/6J wild-type mice	WEHI, maintained in house.
Antibodies	
Anti-Human CD3 (SK7)	BD Biosciences
Anti-Human CD8a (HIT8a)	Biolegend
Anti-Human CD4 (SK3)	Biolegend
Anti-Human CD69 (FN50)	Biolegend
Anti-Human CD226 (11A8)	Biolegend
Anti-Human CD28 (28.2)	Biolegend
Anti-Human/Mouse Granzyme B (GB11)	Biolegend
Anti-Human Perforin (dG9)	Biolegend
Anti-Human CD107a (H4A3)	Biolegend
Anti-Human CD269/BCMA (19F2)	Biolegend
Anti-Human CD360/IL-21R (17A10)	Biolegend
Anti-Human CD155 (SKII.4)	Biolegend
Anti-Human CD112 (TX31)	Biolegend
Anti-Human CD80 (2D10)	Biolegend
Anti-Human CD86 (GL-1)	Biolegend

Mouse IgG1 isotype control (MOPC-21)	Thermo Fisher Scientific
Anti-Human IFN-γ (B27)	Biolegend
Anti-alpha Tubulin Monoclonal Antibody (DM1A), Biotin	Thermo Fisher Scientific
Anti-mouse TCRβ (H57-597)	Biolegend
Anti-mouse Foxp3 (FJK-16s)	Thermo Fisher Scientific
Anti-mouse CD8α (53-6.7)	Biolegend
Anti-mouse CD4 (GK1.5)	Biolegend
Anti-mouse PD-1 (29F.IA12)	Biolegend
Anti-mouse NK1.1 (S17016D)	Biolegend
Anti-mouse CD1d tetramer loaded with PBS-57	NIH Tetramer Core Facility
Anti-mouse CD16/32 (2.4G2)	Prepared in house
***In vivo* antibodies**	
Human anti-BCMA-antiCD3 bispecific antibody	BPS Bioscience
Rat IgG_{2a} isotype control (1-1)	Leinco Technologies, Inc.
anti-mouse CD3/BCMA bispecific antibody	Bristol Myers Squibb, Casey et al. [1]
Reagents, Recombinant Proteins, Assay kits	
Lymphoprep™	STEMCELL Technologies
Red Blood Cell Lysis Solution (10x)	Miltenyi Biotec
Recombinant hIL-2	Tecin Teceleukin
Recombinant hIL-7	CAPSUGEL/Peprotech
Recombinant hIL-12 p70	Biolegend
Recombinant hIL-15	CAPSUGEL/Peprotech
Recombinant hIL-18	Biolegend
Recombinant hIL-21	Biolegend
Recombinant mIL-21	Mittal *et al.* [2]
Xenolight D Luciferin Potassium Salt	PerkinElmer
Concanamycin A	Sigma Aldrich
CellTrace™ Violet Cell Proliferation kit	Thermo Fisher Scientific
Zombie Acqua™ Fixable Viability Kit	Biolegend
Zombie Green™ Fixable Viability Kit	Biolegend

Streptavidin, Alexa Fluor™ 555 conjugate	Thermo Fisher Scientific
EasySep™ Human CD8+ T cell Isolation Kit	STEMCELL Technologies
EasySep™ Human CD4+ T cell Isolation Kit	STEMCELL Technologies
ImmunoCult™ Human CD3/CD28 T Cell Activator	STEMCELL Technologies
Foxp3 Transcription Factor Staining Buffer set	Thermo Fisher Scientific
BD Cytofix/Cytoperm™ Fixation/Permeabilization Kit	BD Biosciences
BD Liquid Counting beads	BD Biosciences
Human Granzyme B DuoSet ELISA	R and D systems
Human Perforin ELISA Set (ab83709)	ABCAM
Human IFN gamma Matched Antibody Pair	Thermo Fisher Scientific
Human ELISA MAX™ Deluxe Set TNF-a ELISA Kit	Biolegend
Human GM-CSF Uncoated ELISA	Thermo Fisher Scientific
RNeasy Plus Micro Kit	Qiagen
TruSeq Stranded mRNA Library Prep	Illumina
Mouse Granzyme B ELISA kit	Thermo Fisher Scientific
Mouse Interferon-γ ELISA kit	Thermo Fisher Scientific
Sebia Hydragel 30 B1-B2	Abacus dx
Cell lines	
JJN-3-GFP	Casey *et al*.[3]
JJN-3-mcherry-luciferase	In this paper
RPMI8226-GFP-luciferase	Casey *et al*.[3]
KMS-11	Vuckovic *et al*.[4]
KMS-11-mcherry-luciferase	In this paper
VK14451-EGFP	Casey *et al*.[1]
RNA-seq data	
RNA-seq count matrix from human CD8 T cells	In this paper **(Supplementary Table 1)**
Software	
Graphpad Prism 9.0 software	GraphPad Software, Inc.
ZEN Microscopy Software	ZEISS
FlowJo™ v10 software	BD Biosciences

Supplementary Methods

RNA sequencing (RNA-seq)

GFP-expressing JJN-3 myeloma cells (2×10^5) and CD8 T cells (8×10^5) isolated from six independent healthy donors were co-cultured and stimulated with anti-BCMA T-BsAb (0.2 µg/ml) in cRPMI supplemented with rIL-2 (20 U/ml) in the absence (control) or presence of rIL-21 (100 ng/ml) using a paired design, where each donor received both control or rIL-21. After 3 days of co-culture, CD8 T cells were sorted by the BD FACS Aria III Cell Sorter. RNA was isolated using the RNeasy Plus Micro Kit from two experimental groups (control and IL-21) with six biological replicates (donors) per group. RNA samples with RIN scores > 8 were selected for cDNA library preparation using the Illumina TruSeq stranded mRNA Library Prep Kit. Libraries were sequenced using the IIlumina NextSeq 2000 platform at the QIMR Berghofer Sequencing Facility with 75 bp paired-end reads. Each sample obtained an average sequencing depth of 41 million reads (range 35.9 – 45.6 million). Sequence reads were trimmed for adapter sequences using Cutadapt version 1.9[5] and aligned using STAR version 2.5.2a[6] to the human genome assembly GRCh37 with the Ensembl release 97 gene model. Quality control metrics were computed using RNA-SeQC version 1.1.8[7] and transcripts were quantified using RSEM version 1.2.30.[8] All downstream RNA-seq analysis was performed with R version 4.2.0,[9] using the expected gene counts output from RSEM **(Supplementary Table 1)**. Differential expression analysis was performed using the quasi-likelihood pipeline from edgeR version 3.40.2.[10-12] Only protein-coding genes that passed edgeR's filterByExpr function were kept for downstream analysis. To normalize data for visualization purposes, effective library sizes were calculated using edgeR's

calcNormFactors function based on the Trimmed mean of M values method and input together with the filtered counts to edgeR's cpm function with log set to TRUE. Z-scores were then calculated from log2-transformed and normalized values using the scale function with center and scale set to TRUE. Principal component analysis was performed using the prcomp function using z-scores as input. The heatmap was constructed based on z-scores using the ComplexHeatmap package version 2.14.0. Raw counts were input to edgeR for differential gene expression analysis. To compare the IL-21 and control groups, we used a design matrix that incorporated a donor term, namely *model.matrix(~Donor + Group)*, where donor represented one of the six donors, and group represented control or IL-21. Differentially expressed genes were determined based on false discovery rate (FDR) < 0.05, with multiple testing correction performed using the p.adjust method "BH". To perform Reactome Pathway enrichment analysis, first we converted DEG gene IDs from Ensembl to Entrez IDs using the bitr function from the clusterProfiler package version 4.6.2.[13] Entrez IDs for up-regulated and down-regulated genes were separately passed to the enrichPathway function from ReactomePA version 1.42.0.[14] Adjusted p-values were calculated using the p.adjust method "BH" (clusterProfiler default), and pathways with an adjusted p-value < 0.05 were considered enriched. The top ten enriched pathways (based on ascending p-value) were visualized using the dotplot function from clusterProfiler.

Cytotoxicity assays

Isolated CD8 T cells were stimulated for 3 days with ImmunoCult™ Human CD3/CD28 T Cell Activator in cRPMI supplemented with rhIL-2 (10 U/ml) alone or in combination with

rIL-21 (100 ng/ml), followed by maintenance in media without stimulation beads for 2 days. After the washout of IL-21, these IL-21-primed CD8 T cells and control CD8 T cells were used as effector cells. In some experiments, control and IL-21-primed CD4 T cells were generated from isolated CD4 T cells. Target myeloma cells expressing luciferase (1×10^5) were co-cultured with effector T cells at indicated ratios, with various concentrations of anti-BCMA T-BsAb. After 4 hours of co-culture, cells were reconstituted with fresh cRPMI containing D-luciferin (150 µg/ml) and incubated for 10 min. Tumor viability was determined by luciferase activities.[15] In some experiments, anti-CD226 blocking mAb (DX11), anti-IFN-γ neutralizing mAb (B27), or control IgG (MOPC-21) were added (5 µg/m) before starting co-culture. For inhibition of perforin, effector CD8 T cells were pre-treated with concanamycin A (50 nM) for 2 hours, followed by washing with media.

Degranulation assays

Control CD8 T cells and IL-21-primed CD8 T cells were co-cultured with RPMI8226 myeloma cells at a 1:1 E: T ratio in the presence of anti-BCMA T-BsAb (0.1 µg/ml) and anti-CD107a (LAMP1) PE-conjugated mAb (clone H4A3, 1:100 in media). Frequencies of CD8 T cells expressing CD107a were determined by flow cytometry at indicated time points.

Confocal microscopy

Control CD8 T cells and IL-21-primed CD8 T cells were labeled with CTV, and co-cultured with GFP-expressing RPMI8226 myeloma cells for 15 min at a 1:1 E:T ratio in the presence of anti-BCMA T-BsAb (0.1 µg/ml). These cells were fixed by image-iT™

Fixative Solutions for 30 min, followed by permeabilization with 0.05% Triton X-100 for 10 min. Then, cells were stained with anti-GFP (Alexa Fluor 488) and anti-α-Tubulin (biotin), followed by streptavidin (Alexa Fluor 555). The distance between the microtubule-organizing center (MTOC) and the center of the contact site was measured, as described previously.[16] Images were acquired by the Zeiss 780-NLO confocal microscopy and analyzed by the ZEN Microscopy Software.

Flow cytometry

Immunostaining of single-cell suspension was performed, as described previously.[1,17] Cell surface staining was performed in the presence of indicated mAbs. Tumor burden was determined by EGFP-positive tumor cells in the femoral BM. The cell numbers of each subset were calculated by counting beads. Samples were acquired by the BD LSR Fortessa Flow Cytometer and analyzed with FlowJo version 10. Cell sorting was performed by the BD FACSAria™ III Sorter.

References

1. Casey M, Tu C, Harrison SJ, Nakamura K. Invariant NKT cells dictate antitumor immunity elicited by a bispecific antibody cotargeting CD3 and BCMA. Blood Adv. 2022;6(17):5165-5170.
2. Mittal D, Caramia F, Michiels S, et al. Improved Treatment of Breast Cancer with Anti-HER2 Therapy Requires Interleukin-21 Signaling in CD8+ T Cells. Cancer Res. 2016;76(2):264-274.
3. Casey M, Lee C, Kwok W, et al. Regulatory T cells hamper the efficacy of T cell-engaging bispecific antibody therapy. Haematologica. 2023; doi: 10.3324/haematol.2023.283758
4. Vuckovic S, Vandyke K, Rickards DA, et al. The cationic small molecule GW4869 is cytotoxic to high phosphatidylserine-expressing myeloma cells. Br J Haematol. 2017;177(3):423-440.
5. Martin M. Cutadapt removes adapter sequences from high-throughput sequencing reads. 2011;17(1):3.
6. Dobin A, Davis CA, Schlesinger F, et al. STAR: ultrafast universal RNA-seq aligner. Bioinformatics. 2013;29(1):15-21.
7. DeLuca DS, Levin JZ, Sivachenko A, et al. RNA-SeQC: RNA-seq metrics for quality control and process optimization. Bioinformatics. 2012;28(11):1530-1532.
8. Li B, Dewey CN. RSEM: accurate transcript quantification from RNA-Seq data with or without a reference genome. BMC Bioinformatics. 2011;12:323.
9. R: A Language and Environment for Statistical Computing. R Core Team (2022), R Foundation for Statistical Computing, Vienna, Austria https://wwwR-projectorg/.
10. Chen Y, Lun AT, Smyth GK. From reads to genes to pathways: differential expression analysis of RNA-Seq experiments using Rsubread and the edgeR quasi-likelihood pipeline. F1000Res. 2016;5:1438.
11. Robinson MD, McCarthy DJ, Smyth GK. edgeR: a Bioconductor package for differential expression analysis of digital gene expression data. Bioinformatics. 2010;26(1):139-140.
12. McCarthy DJ, Chen Y, Smyth GK. Differential expression analysis of multifactor RNA-Seq experiments with respect to biological variation. Nucleic Acids Res. 2012;40(10):4288-4297.
13. Wu T, Hu E, Xu S, et al. clusterProfiler 4.0: A universal enrichment tool for interpreting omics data. Innovation (Camb). 2021;2(3):100141.
14. Yu G, He QY. ReactomePA: an R/Bioconductor package for reactome pathway analysis and visualization. Mol Biosyst. 2016;12(2):477-479.
15. Fu X, Tao L, Rivera A, et al. A simple and sensitive method for measuring tumor-specific T cell cytotoxicity. PLoS One. 2010;5(7):e11867.
16. Bertrand F, Müller S, Roh KH, Laurent C, Dupré L, Valitutti S. An initial and rapid step of lytic granule secretion precedes microtubule organizing center polarization at the cytotoxic T lymphocyte/target cell synapse. Proc Natl Acad Sci U S A. 2013;110(15):6073-6078.
17. Nakamura K, Kassem S, Cleynen A, et al. Dysregulated IL-18 Is a Key Driver of Immunosuppression and a Possible Therapeutic Target in the Multiple Myeloma Microenvironment. Cancer Cell. 2018;33(4):634-648.e635.

Supplementary Figure 1

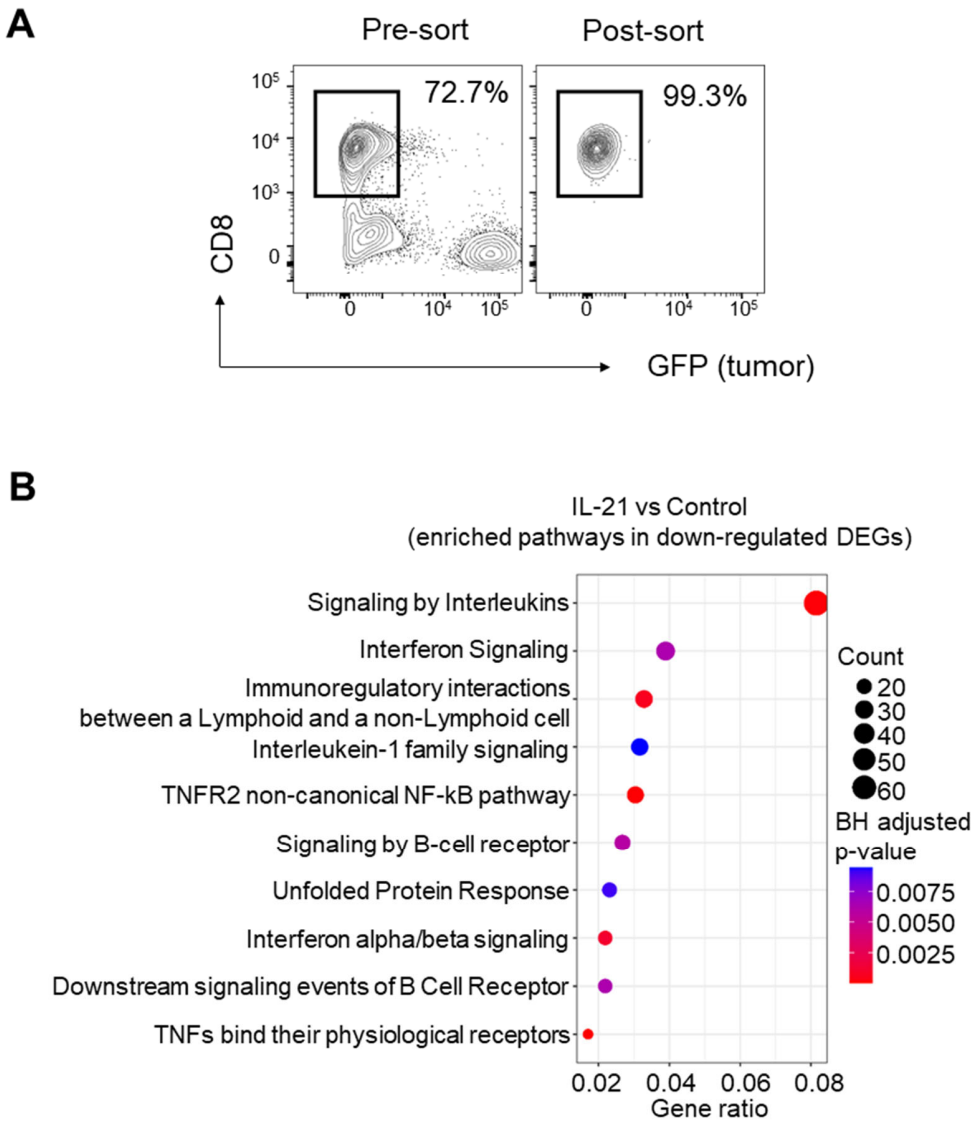

Supplementary Figure 1. RNA-sequencing of CD8 T cells.

(A) Representative flow cytometry plots showing purity of CD8 T cells after cell sorting.

(B) Enriched Reactome pathways in differentially expressed genes (DEGs) significantly downregulated in IL-21-primed CD8 T cells compared with control CD8 T cells.

Supplementary Figure 2

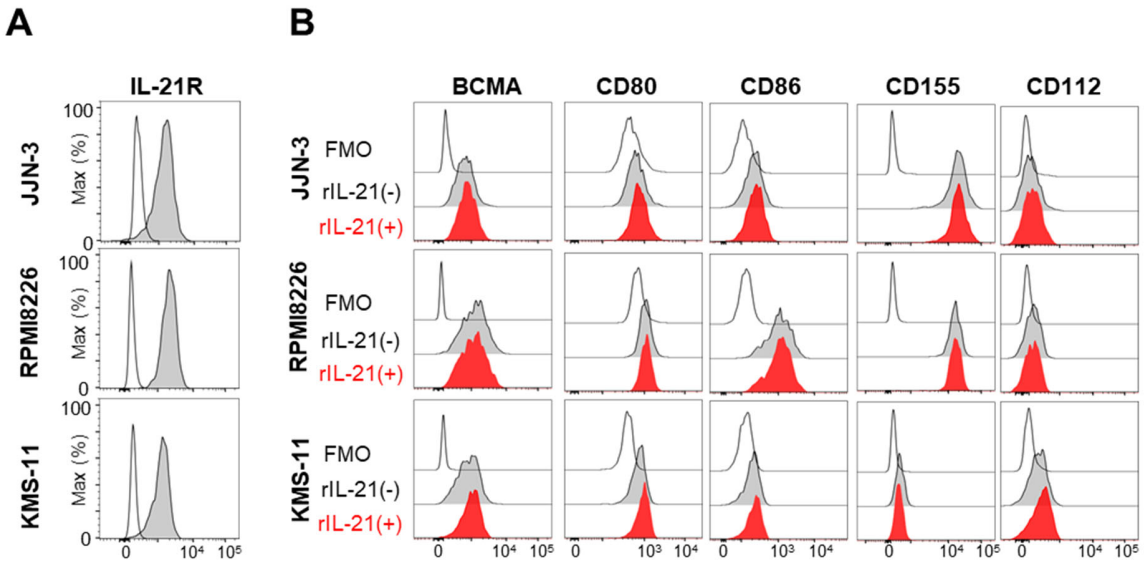

Supplementary Figure 2. The impact of IL-21 on myeloma cells.

(A) Representative histograms showing expression levels of IL-21 receptor on JJN-3, RPMI8226, and KMS-11 myeloma cells.

(B) Indicated myeloma cells were treated with or without rIL-21 (100 ng/ml) for 24 hours. Representative histograms showing the expression level of indicated molecules. FMO indicates fluorescence minus one controls.

Supplementary Figure 3

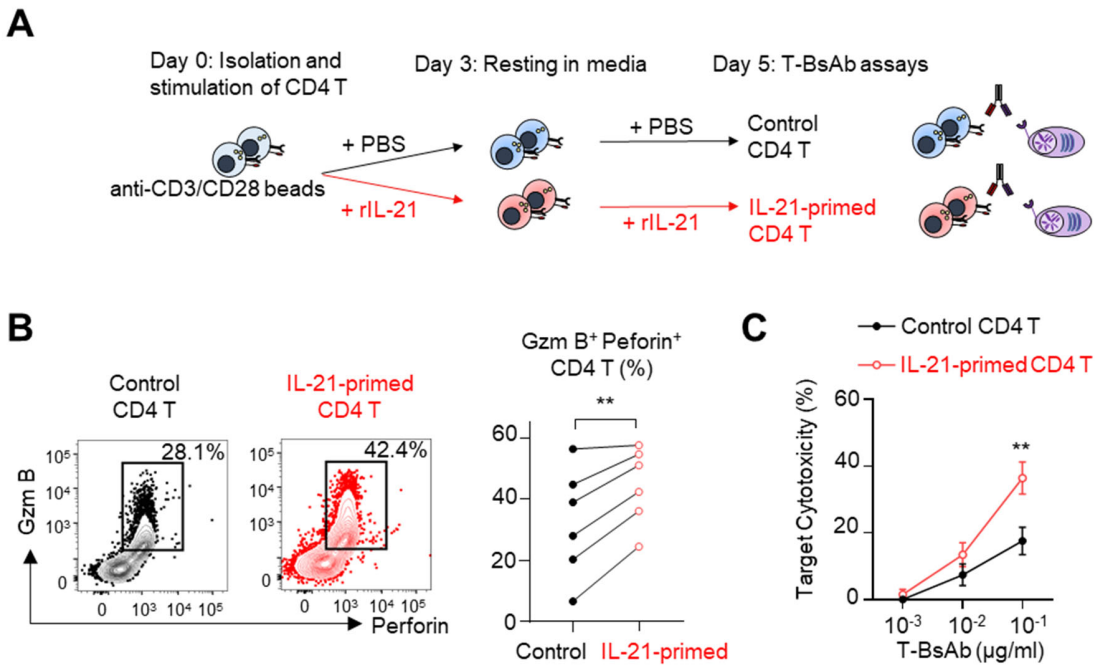

Supplementary Figure 3. IL-21 induces the cytotoxic program in CD4 T cells.

(A) A schematic illustrating preparation of control and IL-21-primed CD4 T cells.

(B) Representative flow cytometry plots and individual graphs showing frequencies of CD4 T cells expressing granzyme B (Gzm B) and perforin in control and IL-21-primed CD4 T cells (n=6).

(C) CD4 T cells were co-cultured with RPMI8226 myeloma cells expressing luciferase at a 4:1 E: T ratio for 4 hours. Graphs showing target cytotoxicity with different concentrations of T-cell-engaging bispecific antibody targeting B-cell maturation antigen (anti-BCMA T-BsAb). Data are shown as mean ± standard error of mean (n=6).

Differences were tested for statistical significance using a paired t-test. **p < 0.01.

Supplementary Figure 4

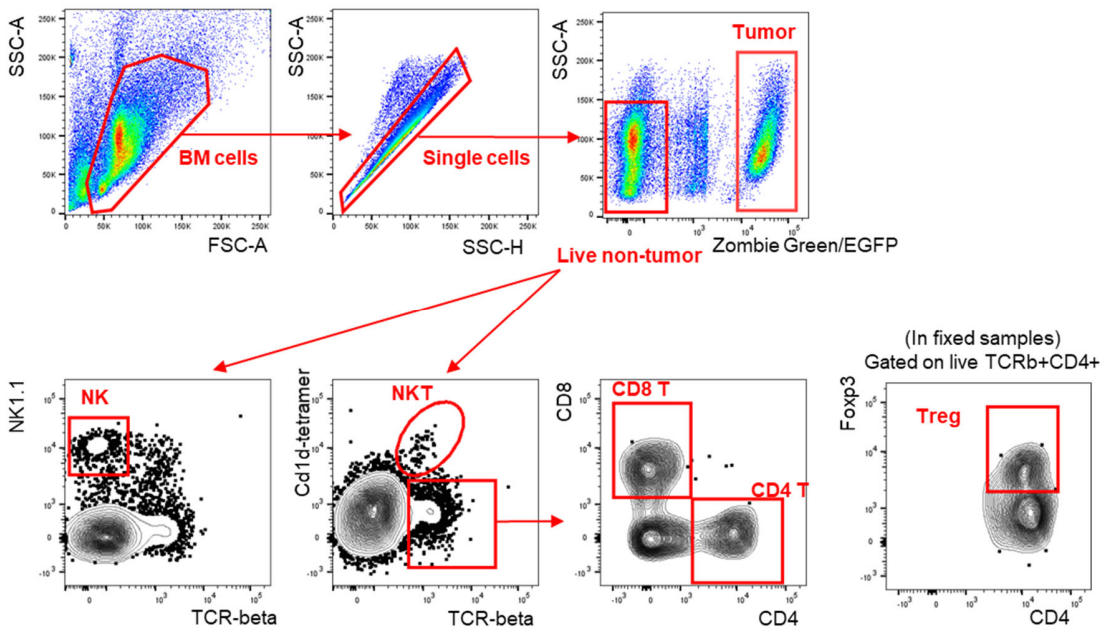

Supplementary Figure 4. Gating strategies in bone marrow cells from tumor-bearing mice.

C57BL/6 wild-type mice were challenged with Vk14451 myeloma cells, and treated with or without rIL-21. Representative flow cytometry plots showing the gating strategy in bone marrow cells.